NANO LETTERS

2001
Vol. 1, No. 12
707−711

(111)-Specific Coalescence Twinning and Martensitic Transformation of Tetragonal ZrO_2 Condensates

P. Shen* and W. H. Lee

Institute of Materials Science and Engineering, National Sun Yat-sen University, Kaohsiung 804, Taiwan, R.O.C.

Received August 7, 2001

ABSTRACT

ZrO_2 nanoparticles (10−400 nm) were produced by laser ablation deposition and studied by transmission electron microscopy. The particles were predominantly tetragonal (t-) phase with spherical shape. Relatively large t-ZrO_2 particles, however, showed {111} and {100} faces and tended to attach over well-developed {111}, hence forming twinned bicrystals. Upon electron irradiation, the t-ZrO_2 particles transformed to monoclinic (m-) phase, at a smaller critical size than that reported in matrix systems, by nucleating from particle surface, in particular at the outcrop of planar defect. Further growth caused {100} or {110} type twin boundary but not closure twins, in contrast with that under the influence of matrix constraint. In situ observations of t−m transformtion for spherical ZrO_2 nanoparticles also enabled shape-change determination, typically dilation and contraction along orthogonal ⟨110⟩ directions and invariant plane strain along (001) twin plane, for this martensitic-type transformation.

In this work, tetragonal (t-) ZrO_2 nanoparticles produced by laser ablation condensation were studied by transmission electron microscopy (TEM) with regard to the coalescence mechanism and the martensitic t- to monoclinic (m-) transformation for the nanoparticles without matrix constraint.

Laser ablation condensation can be used to prepare nanoparticles. The CeO_2-ZrO_2 solid solution condensates prepared by this method predominantly have cubic (c-) fluorite type structure and their shape changes from {111} octahedron, {100}+{111} cubooctahedron to sphere with minor {111} facets as the ZrO_2 content increases.[1,2] The condensates having different shape and size were found to twin over well developed {111} plane indicating a twinning mechanism of coalescence[2] rather than growth, transformation, or deformation.[3] Since the fluorite type structure has an oxygen-terminated {111} surface and *ABC* type stacking sequence of the cations, it was suggested that the crystallites were coalesced over the {111} contact plane by anchorage at specific atomic positions or subject to rigid body rotation within 60° to reach FCC type twin.[2] Coalescence via a solution-precipitation route through a Si-rich liquid phase at a necking area was also suggested for CeO_2-ZrO_2 nanoparticles.[4] In this article, we report further {111}-specific coalescence twinning of t-ZrO_2 condensates almost free of solute and impurities. Most of the present condensates fall into a size regime that has not yet been investigated in much detail and suitable for the study of the coalescence mechanism upon which the nanoparticles become larger and twinned.

Partially stabilized zirconia (PSZ) and zirconia dispersed ceramic (ZDC), both having t-ZrO_2 phase dispersed in a matrix phase, have been extensively studied regarding the effect of matrix constraint on martensitic t−m transformation.[5] In addition to a suppressing effect on the transformation, a matrix constraint was known to cause closure twins as well as {100}+{110} mosaic twins for embedded m-ZrO_2 particles.[6] In general, there is residual compression strain field of the matrix around the embedded m-ZrO_2 particles.[7−9] Shear strain fields also exist in the confined t-ZrO_2 particle[8] due to the anisotropy of the thermal expansion of t-ZrO_2.[10] The study of small t-ZrO_2 particles in Cu matrix[11,12] further indicated that nucleation of m-ZrO_2 phase was often suppressed by the lack of potent defects. So far, less attention was paid to the martensitic transformation of ZrO_2 particles free of matrix constraint. The transformation kinetics and activation energy of constraint-free ZrO_2 particles were studied by X-ray diffraction,[13] and the sintering behavior by TEM;[14] however, the microstructural changes associated with phase transformation were not examined. The original in situ TEM observations of t−m[15] and orthorhombic (o-) to m-ZrO_2[16] martensitic transformations were made for submicron sized and isolated particles prepared by selective oxidation of Zr in Nb-1%Zr alloy and selective etching of

* To whom correspondence should be addressed. FAX 886-7-5254099. E-mail pshen@mail.nsysu.edu.tw.

10.1021/nl010058r CCC: $20.00
Published on Web 10/04/2001

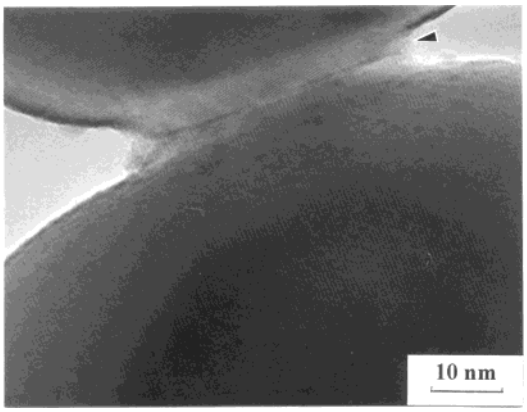

Figure 1. TEM (lattice image) of spherical t-ZrO_2 particles coalesced via ledge growth at the neck area (arrow).

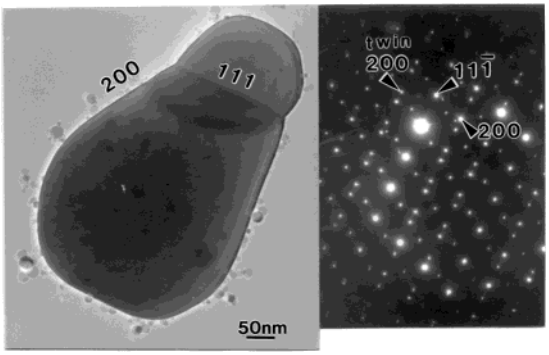

Figure 2. TEM (bright field image, BFI) with inset [011] SAED pattern showing t-ZrO_2 particles twinned over {111} plane as a result of oriented attachment over the {111} surface.

the Nb matrix. This approach circumvents the troublesome effect of matrix constraint as encountered in PSZs and ZDCs. Here we report further in situ TEM observations of smaller and spherical ZrO_2 particles produced by laser ablation condensation that revealed a smaller critical size and more significant shape change for t−m transformation than that reported in matrix systems.

The sintered pellets of ZrO_2 were used as targets for laser ablation deposition. To prepare such pellets, powders of ZrO_2 (Cerac 99.9% pure) were ball milled, dry pressed at 100 MPa into pellets ca. 10 mm in diameter and 3 mm in thickness, and then sintered at 1600 °C for 4 h, followed by cooling in an open air furnace. The target was subject to CO_2-laser (PRC, FH-3000, 10.6 μm in wavelength, beam mode: TEM00+01*) treatments at a specified power input (1600 W) and time period (8 s) in air as adopted previously.[17] Copper grids overlaid with a carbon-coated collodion film was used to collect the condensed materials for TEM observations using a JEOL 3010 instrument operating at 300 kV for both imaging and energy-dispersive X-ray (EDX) analysis. The selected area electron diffraction (SAED) patterns of the t- and m-phase of ZrO_2 were indexed according to the distorted version of the c-fluorite cell as adopted previously.[18]

The ZrO_2 particles produced by laser ablation were 10 nm to 400 nm in size. They were predominantly t-phase and spherical in shape. A spherical shape for ZrO_2 condensate is in accordance with our previous observations of the CeO_2−ZrO_2 condensate,[1,2] showing shape change from octahedron, cubooctahedron to nearly sphere as ZrO_2 content increases. Such spherical t-ZrO_2 particles tended to coalesce with each other, forming ledges but no liquid phase at the neck area (Figure 1). TEM-EDX analysis shows negligible impurities, in particular Si (a potential liquid phase former), for the coalesced ZrO_2 particles.

The relatively large t-ZrO_2 condensates showed {111} and {100} faces (Figure 2) indicating surface energetics, which, in this case, was determined by atomic plane specification, rather than total surface area. These particles tended to impinge over the well-developed {111} surface, thus forming bicrystals with twin plane {111} (Figure 2) analogous to shape-dependent coalescence of CeO_2 condensates with c-fluorite isostructure.[2] Such type of coalescence twinning is supported by the presence of exposed (111) surfaces for twinned bicrystals (Figure 2) and accountable from a crystallographic point of view, as addressed for CeO_2.[2] (Coalescence of CeO_2 crystallites was found to rely also on an irrational contact plane or (∼111) vicinal surface.[2] Under such a circumstance, considerable atom diffusion across structural ledges is required, in contrast to the simple rotation, within 60° clockwise (cw) or counterclockwise (ccw), of {111}-terminated CeO_2 crystallites to twin or single crystal.[2]) The formation of twin boundaries[19] or faults[20] via oriented attachment on specific planes has also been reported for TiO_2 (anatase) nanocrystals prepared in solution. It is noteworthy that for about 50 assembled t-ZrO_2 particles in Figure 2, only the two relatively large ones with exposed {111} surfaces showed {111}-specific coalescence twinning. A small fraction of such occurrences can be explained by the fact that {111} surfaces exist only in larger particles, which somehow grew at expense of attached spherical nanoparticles. Based on three independent observations of such particle assembly, we conclude that only relatively large particles with well-developed {111} faces allow {111}-specific coalescence twinning.

Electron irradiation was effective to induce t−m transformation for relatively large particles. For example, Figure 3a shows a spherical t-ZrO_2 particle (ca. 200 nm in size and a lattice-parameter ratio (c/a) of 1.02 as measured in [100] orientation), which transformed rather quickly to m-phase with significant shape and volume changes (Figure 3b). The dimensionality change was measured to be a 9% increase along [011], 4.5% decrease along [$0\bar{1}1$], and negligible along [001] and [010], as a representative of three independent observations. There was a (001) twin boundary in this transformed particle (Figure 3b), giving rise to a diffraction streak along the reciprocal [001] direction in the inset SAED pattern. The shape change from t-ZrO_2 sphere into m-ZrO_2 ellipsoid with dilation and contraction along orthogonal ⟨110⟩ directions and invariant plane strain along (001) twin plane is in accordance with martensitic type phase transformation. In contrast, such a phenomenon was difficult to characterize for the ZrO_2 particles in PSZ and ZDC systems due to the presence of matrix constraint. In this connection, the transformation of o-ZrO_2 particles of a square-platelet

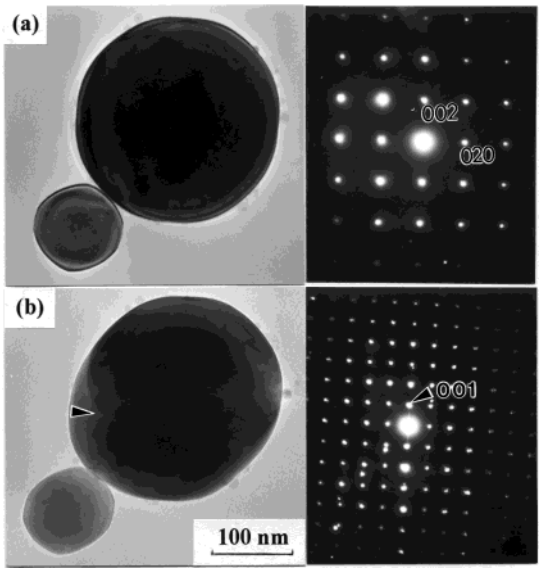

Figure 3. TEM (bright field image) with inset [100] SAED patterns for (a) spherical t-ZrO_2 particle, which transformed upon electron irradiation into (b) m-phase with accompanied shape change from sphere to ellipsoid. Note the (001) twin boundary (arrow) accounts for the diffraction streak in reciprocal space.

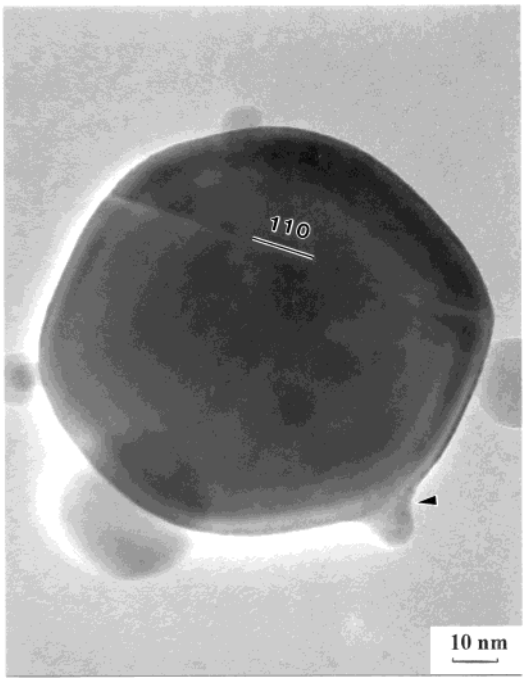

Figure 4. TEM image of electron-irradiation induced m-ZrO_2 particle viewed along [$1\bar{1}1$] zone axis, showing a (110) twin plane across the particle and a coalesced nanoparticle (arrow).

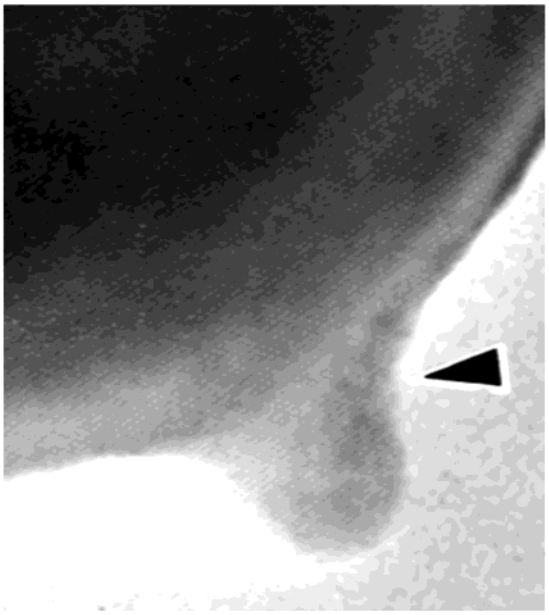

Figure 5. Further magnified view of region near the arrow in Figure 4 to show {110} lattice fringes of m-ZrO_2 extending across the neck area. The fringe interspacing is ca. 0.36 nm.

shape to m-symmetry was found to involve a simple shear plus dilation in the shear plane.[16] Upon electron irradiation, the o/m interface propagated at a speed of 2 nm/s, while maintaining a sharp habit plane, which was stepped on the unit cell scale. The average inclination of this stepped interface also obeyed the invariant plane strain condition.

Figure 4 shows an example of electron-irradiation induced t−m transformation of a nearly spherical ZrO_2 particle about 60 nm in diameter and with a well-coalesced nanoparticle causing (110) twinning and significant shape change of the larger particle as viewed along [$1\bar{1}1$] zone axis. In this case, transformation appeared to start from the surface, propagating across the particle into a coalesced and parallel-oriented particle about 10 nm in diameter, which would otherwise remain t-phase under the influence of nucleation energy barrier in terms of capillarity effect. (Growth via coalescence was manifested by this pair of particles, which could become parallel epitaxy by rotating the smaller particle during laser ablation deposition, or upon electron irradiation as indicated by diffraction contrast change of nanoparticles occasionally occurred during TEM observations.) The region near the arrow in Figure 4 is further magnified in Figure 5 for a clearer view of {110} lattice fringes for the resultant m-ZrO_2 particles. The fringe separations are about 0.36 nm, in agreement with the reported *d* spacings: (110) = 0.3698 nm and (011) = 0.3639 nm for m-ZrO_2 at room temperature (JCPDS file 37-1484). There are no closure twins or appreciable residual strain near the free surface of the transformed particles, in contrast to the case of PSZ and ZDC with effective matrix constraint.[6] Invariant plane strain along the twin plane was again observed for this transformed particle.

When a planar defect, such as that due to oriented attachment of condensates over {111} surface, was present in the particle (Figure 6a), electron-irradiation induced transformation started from the outcrop of the planar defect and grew rapidly to form a (100) twin plate across the particle as shown by the images (Figures 6b and 6c) and SAED pattern (Figure 6d) taken after transformation. Defect-facilitated nucleation has also been reported for the transformation of small ZrO_2 particles embedded in metal and ceramics matrices. For example, the study of ZrO_2 particles in Cu matrix and HfO_2 particles in Ta matrix[11,12] suggested that nucleation was often suppressed by the lack of potent

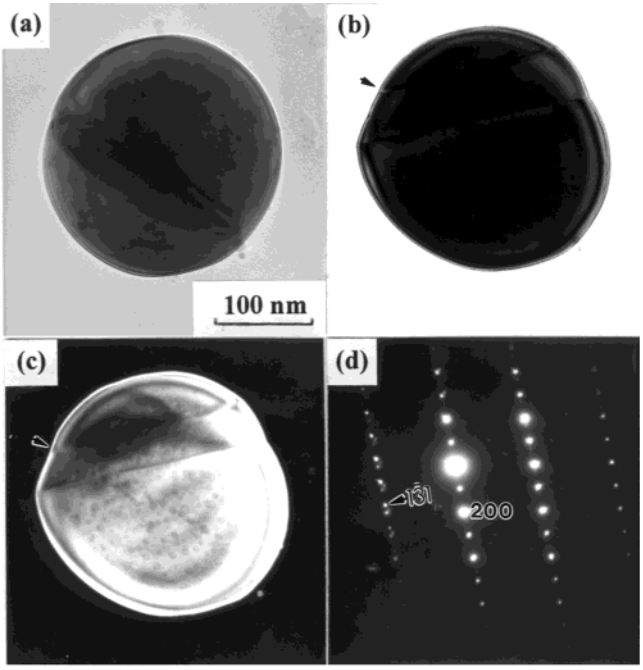

Figure 6. TEM image of electron-irradiation induced t−m transformation of spherical ZrO_2 particle with planar defect. (a) BFI of the particle before transformation. (b) BFI of the particle after transformation. (c) Dark field image using 200 spot shared by m-ZrO_2 twin variants to show more clearly the (100) twin boundary. (d) SAED pattern of the transformed particle in the [013] zone axis.

defects. When such defects are available, nucleation of m-phase occurred spontaneously in the internal stress field of the nucleating defects. It was also proposed that dislocation loops beyond a critical loop size and Hertzian contacts between two particles may cause martensitic nucleation and spontaneous transformation.[15] Oxygen vacancies likely played a negligible role in the martensitic transformation of the present ZrO_2 condensates because no appreciable Zr/O ratio change was detected by EDX analysis after phase transformation. In fact, when oxygen was deficient, as in Zr−ZrO_2 binary system, zirconia tended to stabilize as c- and t-phase[21] and thereby suppress martensitic t−m transformation. It is an open question whether thermal stress as a result of rapid local heating upon electron irradiation caused the martensitic transformation of the ZrO_2 particles.

Crystallographically, there are three possible choices of lattice correspondence, i.e., the *a*, *b*, or *c* axis of m-ZrO_2 to be parallel to the *c* axis of t-ZrO_2. The resultant habit planes of m-twin variants are {100} and {110} for electron-irradiated ZrO_2 condensates (e.g., Figures 4 and 6). The habit planes of m-twinning, either induced by cooling or under the influence of an applied stress, were also reported to be on (100), (001), and (110) for pure ZrO_2 and a number of PSZ and ZDC exhibiting mosaic twins and closure twins.[5,6,22−25] However, an unusual twin plane of {111} was reported for (Fe,Gd)-codoped m-ZrO_2.[26] It was proposed that the point defects caused by dissolution of Fe^{3+} and Gd^{3+} ion in t-ZrO_2 may possibly form clusters to weaken the {111} plane of the t-ZrO_2 phase, making it feasible for crystallographic shear to occur along {111}.

Upon cooling or under the influence of an applied stress, the critical particle size for t−m transformation is around 1 μm for ZrO_2 particles embedded in ceramic matrices.[6] Our recent study of octahedral shaped t-ZrO_2 particles embedded in a MnZn ferrite matrix indicated a critical size of ca. 2.5 μm,[27] but 1.5 μm when a critical magnetic field (between 40 and 60 kOe) was applied to induce magnetostriction of the ferrite matrix.[28] By contrast, the present t-ZrO_2 condensates have a much smaller critical size, less than 60 nm, thus supporting the idea that matrix constraint is effective to suppress the t−m transformation. Since nucleation of m-phase is facilitated by the presence of defects,[11,12] a critical size above which the transformation proceeds can be rationalized by the presence of defects in relatively large particles in addition to the capillarity effect.

In conclusion, laser ablation of polycrystalline ZrO_2 targets caused the condensation of t-ZrO_2 crystallites, mostly spherical in shape but larger ones with {111} and {100} faces. The faceted t-ZrO_2 particles tended to twin over a well-developed {111} plane due to a twinning mechanism of coalescence. Electron irradiation was effective to induce t−m martensitic transformation of spherical condensates at a critical size smaller than that reported in matrix systems, causing significant shape change, e.g., with dilation and contraction along orthogonal ⟨110⟩ directions and invariant plane strain along (001) twin plane, but no closure twins.

Acknowledgment. We thank an anonymous referee for constructive comments. This research was supported by National Science Council, Taiwan, ROC under contract NSC89-2216-E110-013.

References

(1) Kuo, L. Y.; Shen, P. *Mater. Sci. Eng., A* **2000**, *277*, 258.
(2) Lee, W. H.; Shen, P. *J. Cryst. Growth* **1999**, *205*, 169.
(3) Buerger, M. J. *Am. Mineral.* **1945**, *30*, 469.
(4) Lee, W. H.; Shen, P. *Adv. Powder Technol.* **1999**, *10*, 383.
(5) Green, D. J.; Hannink, R. H. J.; Swain, M. V. *Transformation Toughening of Ceramics*; CRC Press: Boca Raton, FL, 1989.
(6) Rühle, M.; Bischoff, E.; Claussen, N. In *Solid-Solid Phase Transformations*; Aaronson, H. I., Laughlin, D. E., Sekerka, R. F., Wayman, C. M., Eds.; Metallurgical Society of AIME: Warrendale, PA, 1982; p 1563 and references therein.
(7) Rühle, M.; Kriven, W. M. In *Solid-Solid Phase Transformations*; Aaronson, H. I., Laughlin, D. E., Sekerka, R. F., Wayman, C. M., Eds.; Metallurgical Society of AIME: Warrendale, PA, 1982; p 1569.
(8) Kriven, W. M. In *Science and Technology of Zirconia II, in Advances in Ceramics, Vol. 12*; Claussen, N., Rühle, M., Heuer, A. H., Eds.; American Ceramic Society: Columbus, OH, 1984; p 64.
(9) Shen, P.; Chen, S.; Chang, W. S. *Mater. Sci. Eng., A* **1994**, *184*, L5.
(10) Patil, R. N.; Subbarao, E. C. *J. Appl. Crystallogr.* **1969**, *2*, 281.
(11) Chen, I. W.; Chiao, Y. H. In *Science and Technology of Zirconia in Advances in Ceramics, Vol. 12*; Heuer, A. H., Hobbs, L. W., Eds.; American Ceramic Society: Columbus, OH, 1984; p 33.
(12) Chen, I. W.; Chiao, Y. H. *Acta Metall.* **1983**, *31*, 1627.
(13) Li, M.; Chi, Z. In *Science and Technology of Zirconia III, Advances in Ceramics, Vol. 24B*; Somiya, S., Yamamoto, N., Yanagida, H., Eds.; American Ceramic Society: Westerville, OH, 1981; p 243.
(14) Rankin, J.; Sheldon, B. W. *Mater. Sci. Eng. A* **1995**, *204*, 48.
(15) Chen, I. W.; Chiao, Y. H. *Mater. Res. Soc. Symp. Proc.* **1987**, *57*, 149.
(16) Chiao, Y. H.; Chen, I. W. *Acta Metall. Mater.* **1990**, *38*, 1163.
(17) Chen, Z. H.; Ho, N. J.; Shen, P. *Mater. Sci. Eng., A* **1995**, *196*, 253.
(18) Teufer, G. *Acta Crystallogr.* **1962**, *15*, 1187.
(19) Penn, R. L.; Banfield, J. F. *Science* **1998**, *281*, 969.
(20) Penn, R. L.; Banfield, J. F. *Am. Mineral.* **1998**, *83*, 1077.

(21) Ruh, R.; Garrett, H. J. *J. Am. Ceram. Soc.* **1967**, *50*, 257.
(22) Wolten, G. M. *J. Am. Ceram. Soc.* **1963**, *46*, 418.
(23) Bailey, J. E. *Proc. R. Soc. London, Ser. A* **1964**, *279*, 395.
(24) Bansal, G. K.; Heuer, A. H. *Acta Metall.* **1972**, *20*, 1281.
(25) Bansal, G. K.; Heuer, A. H. *Acta Metall.* **1974**, *22*, 409.
(26) Wu, M. L.; Shen, P.; Gan, D. *Mater. Sci. Eng., A* **2001**, *297*, 124.
(27) Lin, Y. C.; Gan, D.; Shen, P. *Mater. Sci. Eng. A* **1994**, *188*, 327.
(28) Lin, Y. C.; Shen, P.; Gan, D. *J. Am. Ceram. Soc*. **1996**, *79*, 559.

NL010058R